Ultrahigh-energy sodium ion capacitors enabled by enhanced intercalation pseudocapacitance of self-standing $Ti_2Nb_2O_9$/CNF anodes

Liaona She[1, 2], Feng Zhang[1], Congying Jia[1], Liping Kang[1], Qi Li[1], Xuexia He[1], Jie Sun[1], Zhibin Lei[1], Zong-Huai Liu[1]*

[1] Key Laboratory of Applied Surface and Colloid Chemistry (Shaanxi Normal University), Ministry of Education, Xi'an, 710062, P. R. China; Shaanxi Key Laboratory for Advanced Energy Devices; Xi'an, 710119, P. R. China; School of Materials Science and Engineering, Shaanxi Normal University, Xi'an, 710119, P. R. China.

[2] Institute of Science and Technology for New Energy, Xi'an Technological University, Xi'an, 710021, P. R. China.

*Correspondence should be addressed to:

Prof. Zong-Huai Liu

School of Materials Science and Engineering, Shaanxi Normal University

Xi'an, Shaanxi, 710062, P. R. China

Tel: ++86-29-81530706

Fax: ++86-29-81530702

E-mail: zhliu@snnu.edu.cn

ORCID iD：0000-0003-4263-0628

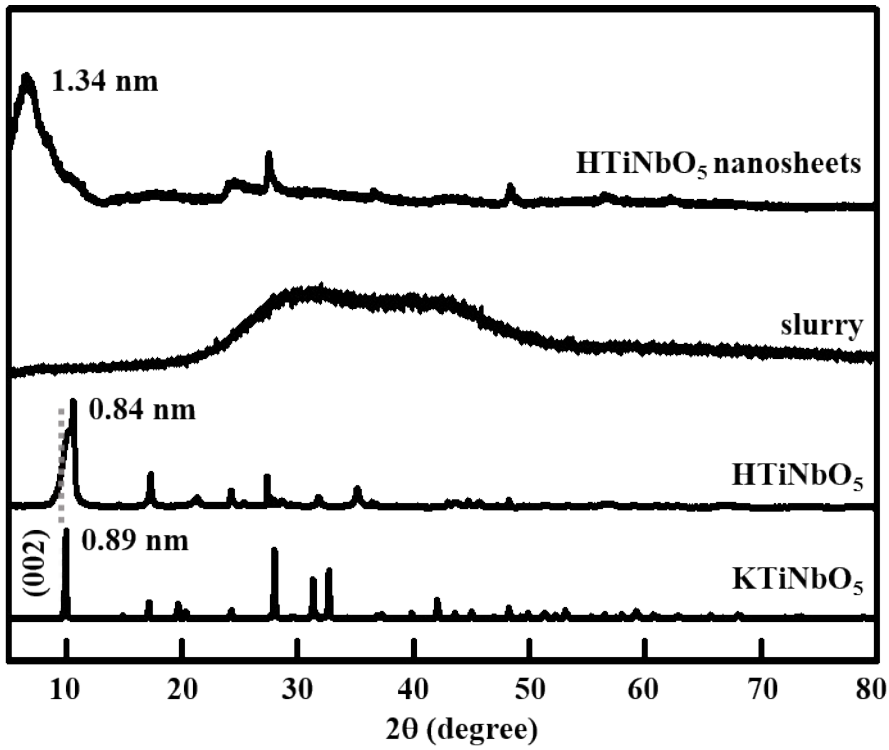

Fig. S1. XRD patterns of bulk $KTiNbO_5$, bulk $HTiNbO_5$, delaminated $HTiNbO_5$ slurry, and $HTiNbO_5$ nanosheets.

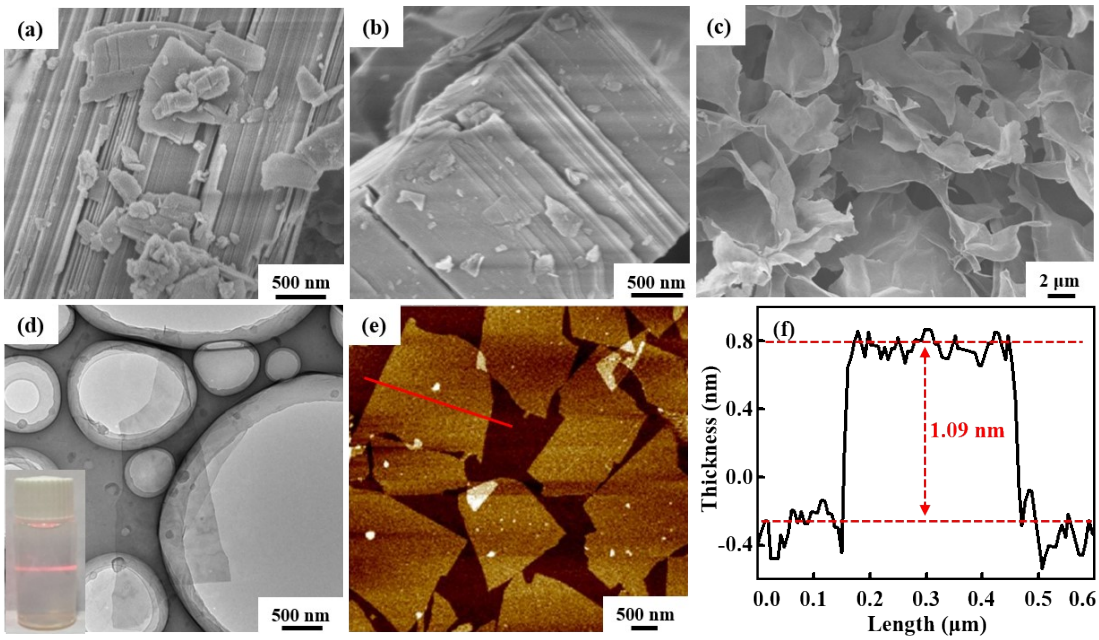

Fig. S2. FE-SEM images of bulk $KTiNbO_5$ (a), bulk $HTiNbO_5$ (b), $HTiNbO_5$ nanosheets (c), TEM image (inserted for the delaminated $HTiNbO_5$ nanosheets suspension) (d), AFM image (e), and the thickness profile (f) of the delaminated $HTiNbO_5$ nanosheets.

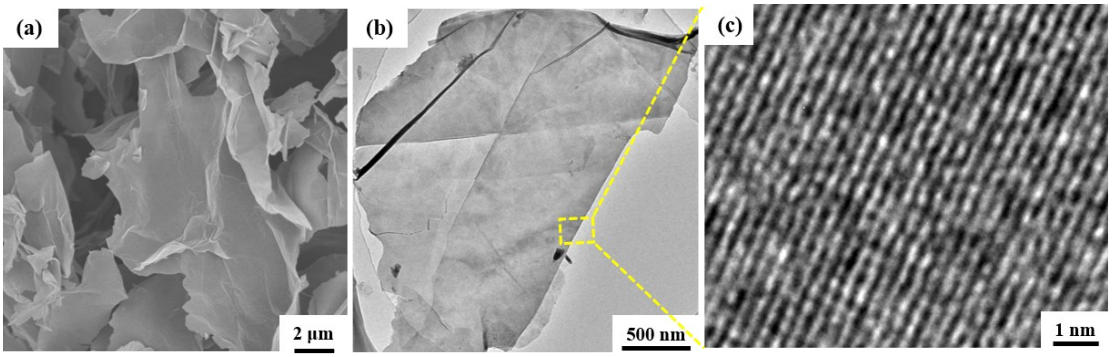

Fig. S3. SEM (a), TEM (b), and HRTEM (c) images of $Ti_2Nb_2O_9$.

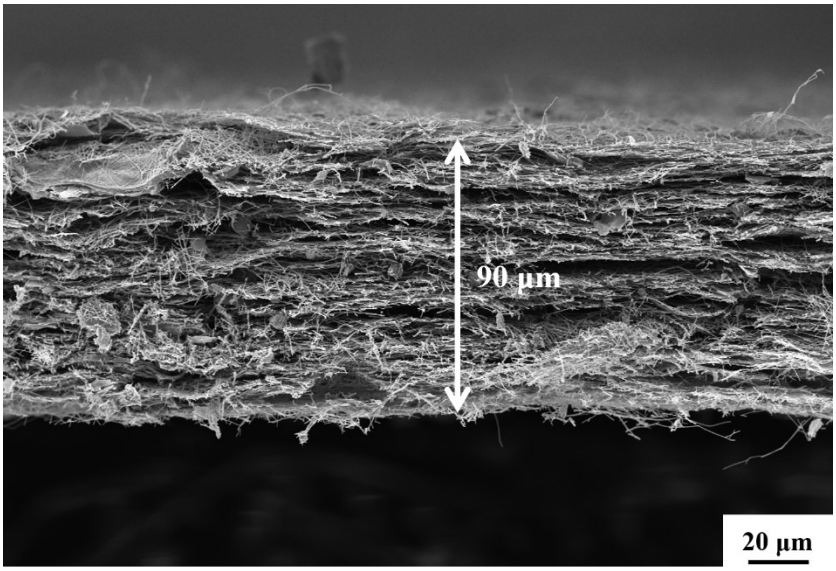

Fig. S4. Cross-sectional morphology of $Ti_2Nb_2O_9$/CNF film.

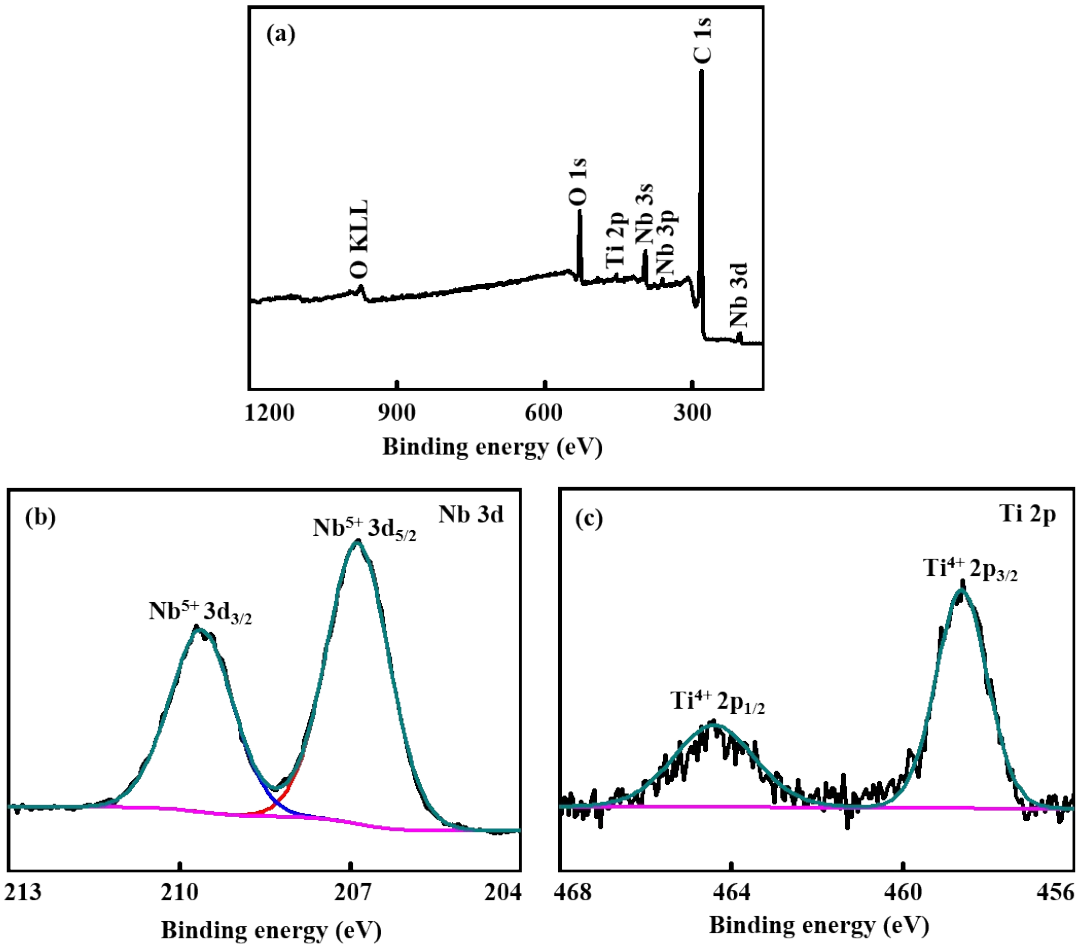

Fig. S5. XPS spectra of $Ti_2Nb_2O_9$/CNF film: survey spectrum (a), high-resolution Nb 3d (b), and Ti 2p (c).

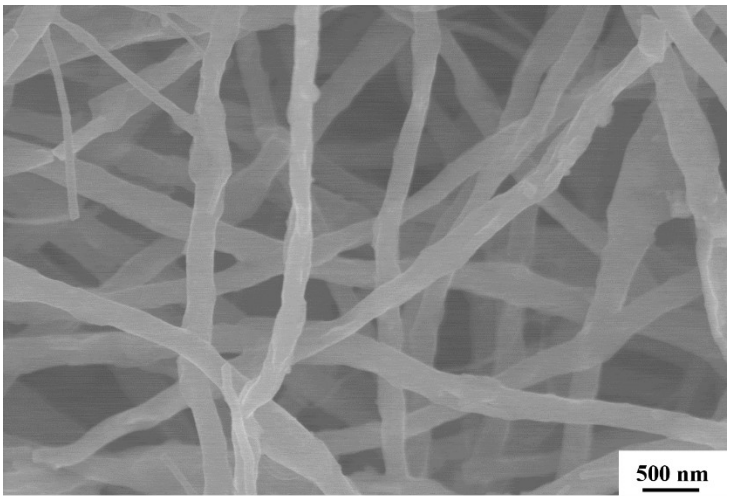

Fig. S6. SEM image of $Ti_2Nb_2O_9$/CNF electrode after 2000 cycles at 1 A g^{-1}.

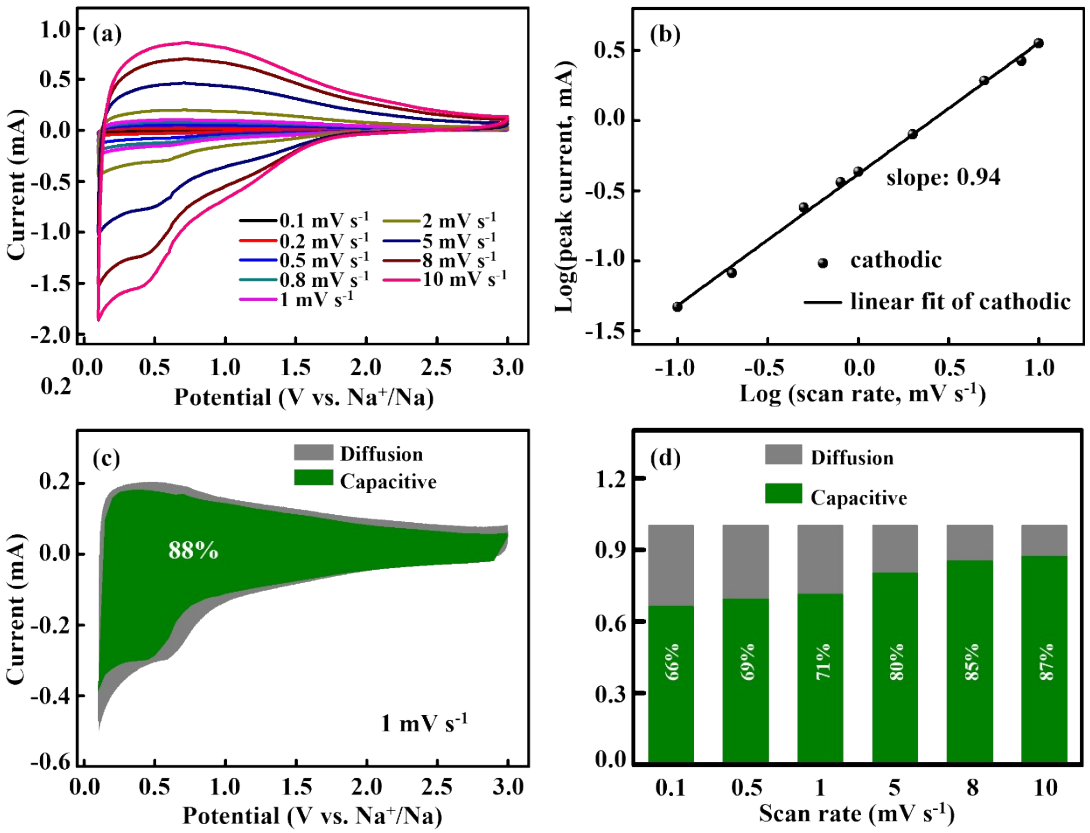

Fig. S7. CV curves at different scan rates (a) and b-value calculated through cathodic scan and peak currents (b) of $Ti_2Nb_2O_9$ electrode, the capacitive and diffusive contribution to the current density at 1 mV s^{-1} of $Ti_2Nb_2O_9$/CNF electrode (c), and capacitive-controlled contribution at different scan rates (d) of $Ti_2Nb_2O_9$ electrode.

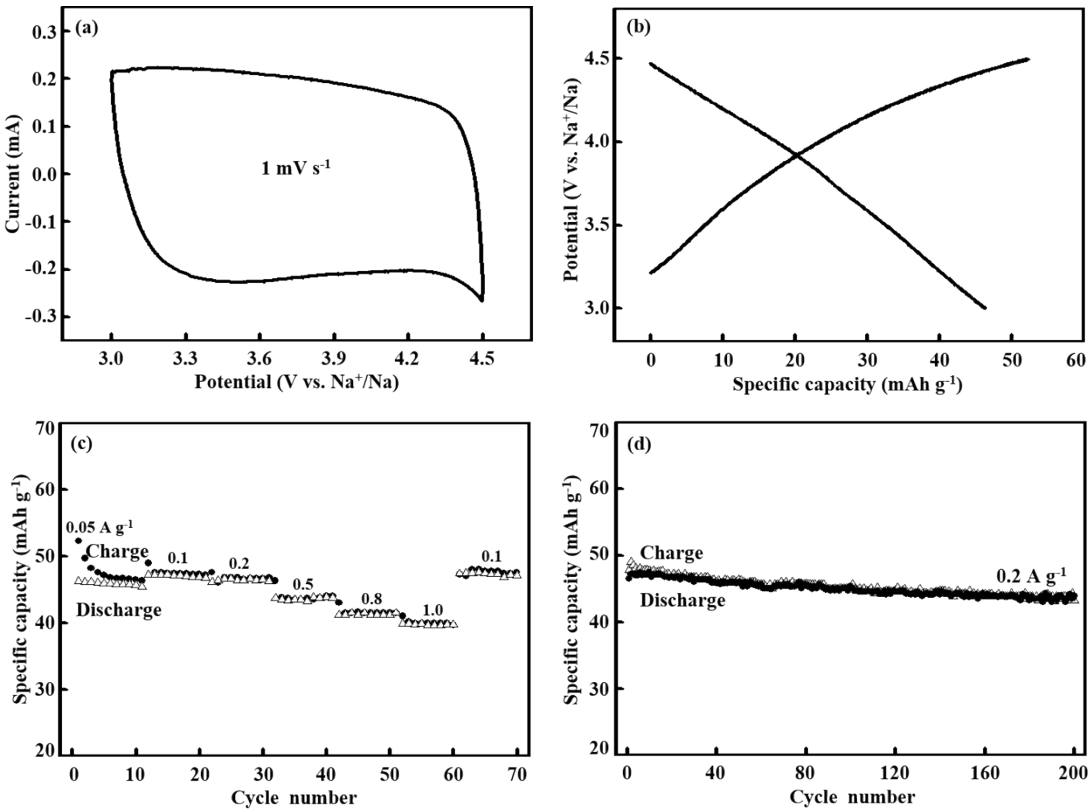

Fig. S8. CV curve at 1 mV s^{-1}(a), galvanostatic charge and discharge curves at 0.05 A g^{-1}between 3.0-4.5 V(b),rate capability at different currentdensities (c), and cycling stability at 0.2 A g^{-1} (d) ofAC electrode.

The quasi-rectangular CV curve at 1 mV s^{-1} and linear GCD curves at 0.05 A g^{-1} indicate electric double-layer capacitive behavior of AC electrode. Its specific capacity at 0.05 A g^{-1} is estimated to be 46 mAh g^{-1}, with outstanding rate capability and good cycling stability at 0.2 A g^{-1} (≈95 % after 200 cycles).

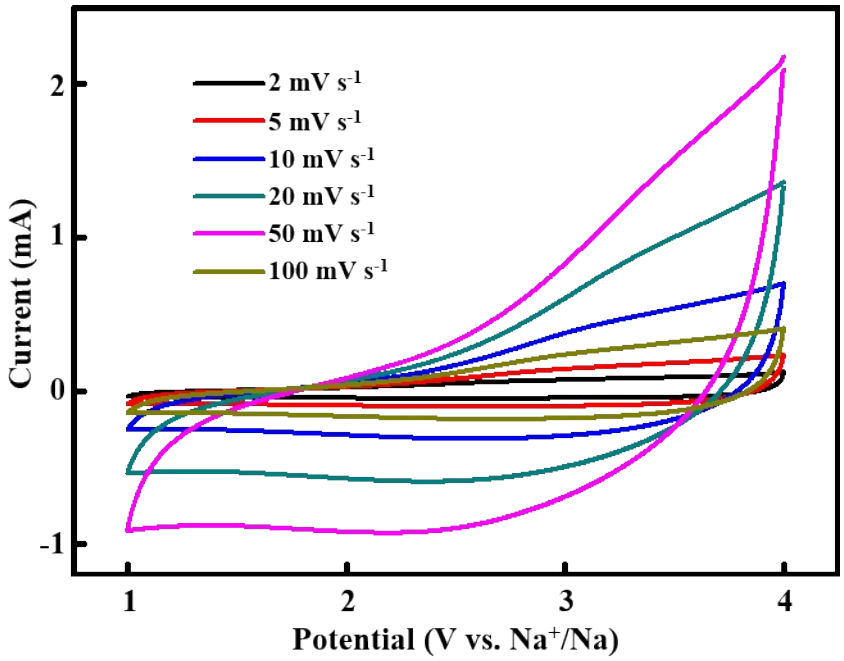

Fig. S9. CV curves at different scan rates from 2 to 100 mV $s^{-1}$of $Ti_2Nb_2O_9$/CNF//AC SIC.